Pré-Publicações do Departamento de Matemática
Universidade de Coimbra
Preprint Number 17–17

A VARIATIONAL MODEL FOR IMAGE ARTIFACT CORRECTION BASED ON WASSERSTEIN DISTANCE

ISABEL NARRA FIGUEIREDO, LUÍS PINTO, GIL GONÇALVES AND BJÖRN ENGQUIST

Abstract: Uneven illumination is a recurrent problem in image processing. This is essentially due to image acquisition sensors' malfunction or external interference. In this paper we propose a variational model for nonuniform illumination correction, that incorporates a penalty term that performs the intensity distribution transfer between two pre-defined sub-regions of the input scalar image, one uniformly illuminated and the other nonuniformly illuminated. This term representing the illumination correction is a Wasserstein distance. It corresponds to the optimal permutation minimizing the cost of rearranging the intensity distribution of the nonuniformly illuminated sub-region into the other, the uniformly illuminated. Simultaneously, this variational model also carries out a regularization of the image by means of a total variation penalty term, to reduce noise. The effectiveness of the model is illustrated for some images.

Keywords: variational model, Wasserstein distance, gradient descent, uneven illumination correction.
AMS Subject Classification (2010): 68U10, 65M06, 49K20.

1. Introduction

Nonuniform illumination correction, contrast enhancement, color modification and shadow removal are common problems in image processing. In particular medical imagery [3] as well as remote sensing imagery [5] are frequently affected by these type of problems. These are errors that are caused by faults or lack of accuracy of the acquisition devices or by external factors, as for example, properties of the organ under study, in the case of medical images, or, in the case of remote sensing images, atmospheric scattering or absorption, terrain attenuation, aspect, clouds, variability of light conditions, and so on. Uniform illumination is an extremely important asset to performing correctly other tasks in image processing or image analysis, as for

Received March 14, 2017.
The first two authors acknowledge support from CMUC (UID/MAT/00324/2013 funded by the Portuguese Government through FCT/MCTES and co-funded by the European Regional Development Fund through Partnership Agreement PT2020). Luís Pinto was also supported by FCT scholarship SFRH/BPD/112687/2015.

instance, image registration, image segmentation, classification, detection of abnormalities in medical images, surveillance, etc.

Therefore illumination correction is an important area in image processing and many methods exist in the literature to address it. Among them we refer to histogram equalization techniques [10, 9, 12], which have some drawbacks because they can also generate extra artifacts, and to the very popular and effective PDEs (partial differential equations) based models and variational techniques [2], as for instance [4, 5, 7] relying on the retinex theory [6].

In this paper, and motivated by the variational model described in [13], as well as in [11], we propose a simple and alternative variational model for artifact correction in scalar images, involving the Wasserstein distance (also called the earth mover distance), which is simultaneously an intensity distribution transfer model and a denoising model. More precisely, it is formulated as a minimization problem, and includes a fidelity term, for preserving the main global features of the image, and two penalty terms: a total variation term representing the denoising technique, while preserving the edges in the image [14], and a Wasserstein metric term that measures the intensity difference between two pre-defined sub-regions of the image, one uniformly and other nonuniformly illuminated. This latter term, relying on the Monge-Kantorovich optimal mass transport theory [15], corrects the badly illuminated parts in the image by changing its pixel intensity distribution in order to match a pre-defined intensity distribution, that in our model corresponds to another pre-defined part, of the same input image, displaying uniform illumination.

The paper is organized as follows. After this introduction, in Section 2 we describe the model and its numerical approximation. In Section 3 we present the tests to assess the performance of the model and the results obtained. The paper ends with some conclusions and perspectives.

2. Variational Model

Let $u : \Omega \to [0, 255]$ denote a generic discrete grayscale image with Ω a discrete two-dimensional set of size $n_1 \times n_2$ and where $x \in \Omega$ denotes the coordinates of an arbitrary pixel. The real value $u(x) \in [0, 255]$ is usually referred to as the intensity of pixel x.

Let us denote by I_o the original noise free image, by I_n the noisy input image, and by I_r a reference image to be defined later on. We define the

following variational model

$$\min_u \Big(\theta F(u, I_n) + \alpha TV(u) + \beta(x) W(u, I_r)\Big), \tag{1}$$

where $F(\cdot,\cdot)$ represents a fidelity term, given by,

$$F(u, I_n) = \frac{1}{2}\sum_{x\in\Omega}(I_n(x) - u(x))^2\, dx, \tag{2}$$

$TV(\cdot)$ denotes the total variation penalty term, defined by,

$$TV(u) = \sum_{x\in\Omega}(\nabla_{x_1} u(x)^2 + \nabla_{x_2} u(x)^2)^{1/2}, \tag{3}$$

with ∇_{x_1} and ∇_{x_2} are discrete versions of the vertical and horizontal derivatives, respectively. In (1), we also represent by $W(\cdot,\cdot)$ the discrete Wasserstein distance

$$W(u, I_r) = \min_{\sigma\in\Sigma(\Omega)} \frac{1}{2}\sum_{x\in\Omega}(I_r(\sigma(x)) - u(x))^2, \tag{4}$$

where σ is a permutation in the set $\Sigma(\Omega)$ of permutations of Ω. Moreover, still in (1), θ and α are positive parameters while $\beta(x)$ represents a properly defined spatially adaptive term.

For discrete one dimensional settings it is well known [13] that the optimal permutation σ^*, *i.e.*, the solution of the minimization problem (4), can be obtained as the following composition

$$\sigma^* = \sigma_{I_r} \circ \sigma_u^{-1},$$

with σ_u and σ_{I_r} the permutations that sort the pixels of u and I_r in the same order. Using this notation, we can rewrite (4), as follows

$$W(u, I_r) = \frac{1}{2}\sum_{x\in\Omega}(I_r(\sigma^*(x)) - u(x))^2. \tag{5}$$

The problem of sorting $N = n_1 \times n_2$ pixels can be quickly solved in only $O(N \log N)$ operations. However, we note that a straightforward extension of the Wasserstein distance to three dimensional color images is a much more costly problem with at least $O(N^{2.5} \log N)$ time complexity. Recently, in [1], the authors were able to significantly reduce this computational cost by approximating the Wasserstein distance by the so-called Sliced Wasserstein distance. For smoother data there is also the possibility of basing the the

calculation of the Wasserstein distance on the Monge-Ampère equation with linear complexity in practice [8].

To solve the minimization problem (1) we deduce the associated Euler-Lagrange equation (first-order condition) for u, parametrize the descent direction by an artificial time $t \geq 0$ (by considering the image u is a function of space and time) and use an explicit time scheme, to obtain the following numerical implementation

$$\begin{aligned}\frac{u^{n+1}-u^n}{\Delta t} &= \theta \sum_{x\in\Omega}(I_n(x)-u^n(x)) + \beta(x)\sum_{x\in\Omega}(I_r(\sigma^*(x))-u^n(x)) \\ &+ \alpha \sum_{x\in\Omega}\Big(\nabla_{x_1}\Big(\frac{\nabla_{x_1}u^n(x)}{\|\nabla u^n(x)\|_\epsilon}\Big)+\nabla_{x_2}\Big(\frac{\nabla_{x_2}u^n(x)}{\|\nabla u^n(x)\|_\epsilon}\Big)\Big), \quad \text{for } n=0,\ldots,N,\end{aligned} \tag{6}$$

where Δt is the time step parameter and

$$\|\nabla u^n(x)\|_\epsilon = (\epsilon^2 + \nabla_{x_1}u(x)^2 + \nabla_{x_2}u(x)^2)^{1/2},$$

with ϵ a small positive constant added to avoid possible divisions by zero [16]. As an initial condition we take $u^0 = I_n$ and at the boundary we impose Neumann boundary conditions.

3. Numerical Experiments

In this section we present a set of experimental tests that illustrate the behavior of the proposed variational image model (1). We consider artifacts free images, denoted by I_o, and we synthetically generate corrupted images by adding Gaussian noise and illumination distortion to obtain I_n. Two examples with different levels of noise and illumination distortion are given. In this synthetic setting, where the original image I_o is available, we use a brute-force search optimization procedure to find the optimal parameters θ and α. In particular, we look for the parameters combination that minimizes the Euclidean distance between u and I_o, i.e., we solve the following minimization problem

$$\min_{\theta,\alpha}\sum_{x\in\Omega}\big(I_o(x)-u(x)\big)^2,$$

with u the solution, for a particular combination of θ and α, obtained from (6). In what concerns $\beta(x)$, it is obtained from the synthetic mask used to add the illumination distortion.

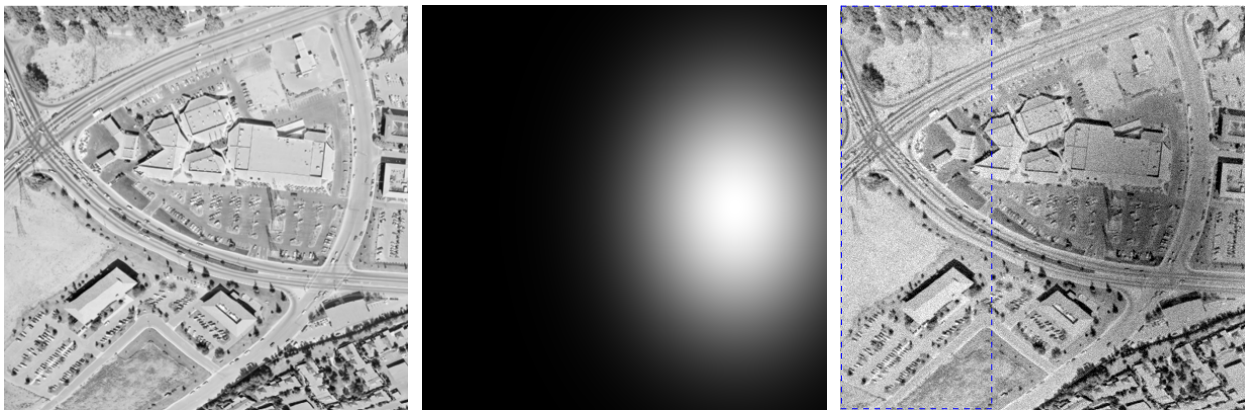

FIGURE 1. From left to right: Original image I_o, intensity distortion mask M_n, and noisy image I_n, where the dashed blue box represents I_r before being resized.

3.1. Example 1. For the first example we consider the original aerial image I_o displayed in Figure1 (on the left). The noisy image I_n, also displayed in Figure 1 (on the right), was obtained from the image I_o by adding Gaussian noise with null mean and variance equal 0.002. Moreover, we used the image M_n (on the middle in Figure1) to apply illumination distortion. For that the following operation was performed

$$I_n = \max(I_o - \gamma M_n, 0) \tag{7}$$

where γ represents the level of distortion, in this case we considered $\gamma = 90$. Note also that $M_n(x) \in [0, 1]$. The parameter $\beta(x)$ is set equal to M_n. This choice means that more weight is given to the Wasserstein term when the illumination distortion is bigger.

The results of the proposed method are given in Figure 2. A close analysis of the recovered image u (image on the left) reveals that the illumination distortion was eliminated and that the level of noise was reduced. Moreover, a comparison with the original image I_o shows that the original contrast was preserved and that the image is not blurred, *i.e.*, the image details have been preserved. The zoom images in Figure 2 confirm this observation. For better illustration we also give in Figure 3 the difference, in absolute value, between the original image I_o and the noisy image I_n (image on the left), and between the original image I_o and the image u obtained with the proposed algorithm (image on the right). As can be seen the recovered image u is much closer than I_n to the original image I_o, a great amount of artifacts (noise and

FIGURE 2. From left to right: image u obtained with the proposed method and zoom image of the recovered image u, noisy image I_n, and original image I_o.

illumination related) were eliminated. For this example the optimal value of the parameters was found to be $\theta = 0.02$ and $\alpha = 0.3$.

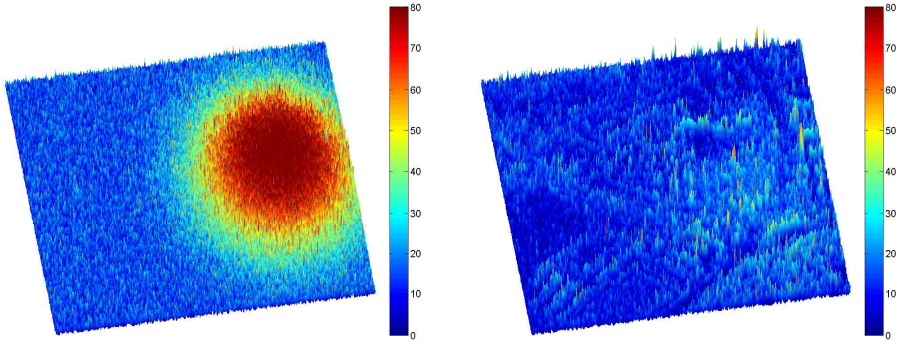

FIGURE 3. From left to right: image of the absolute error between the original image I_o and the noisy image I_n and between the original image I_o and the recovered image u.

3.2. Example 2. In our second example (Mandrill image), the level of noise was increased, we added Gaussian noise with null mean and variance equal 0.01, and the illumination distortion was also stronger, we took $\sigma = 100$ in (7). The image I_o, the image M_n, and the noisy image I_n are presented in Figure 4.

The recovered image u is shown in Figure 5 and even under this more demanding conditions we were able to obtain a good approximation of the original image. As highlighted in the zoom images of Figure 5 much of the

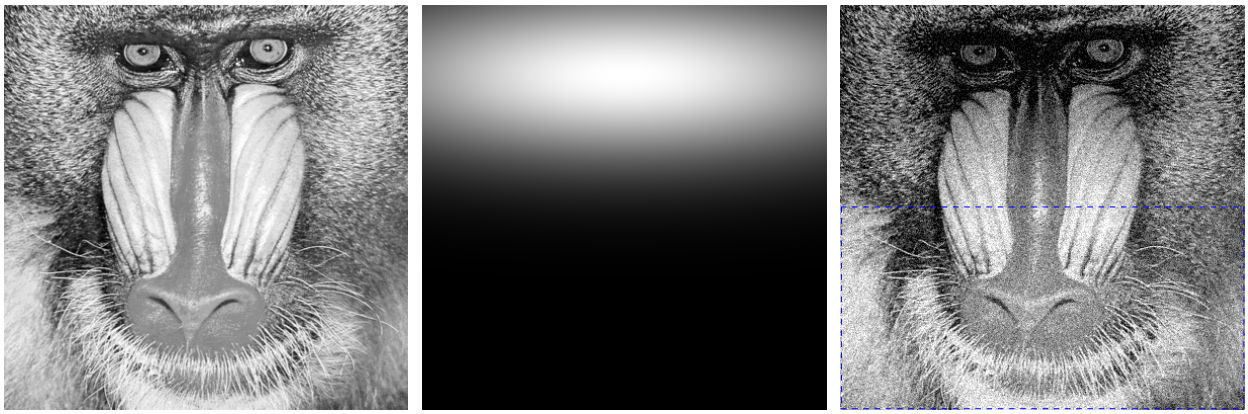

FIGURE 4. From left to right: Original image I_o, intensity distortion mask M_n, and noisy image I_n, where the dashed blue box represents I_r before being resized.

noise and illumination distortion were successfully eliminated and the details were preserved.

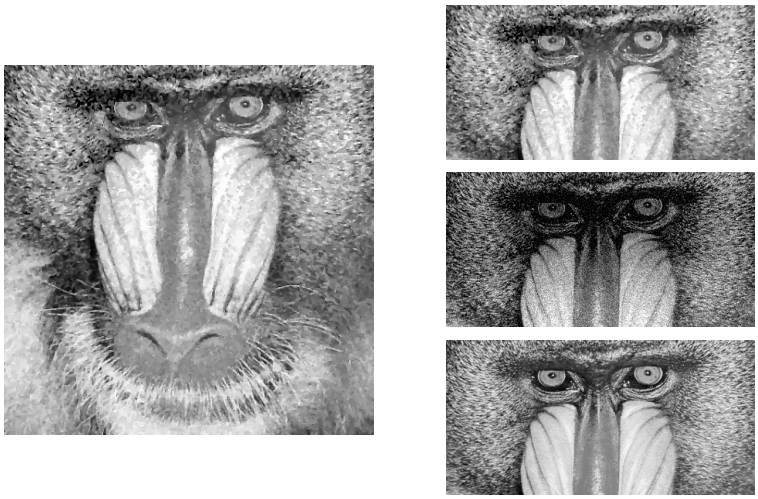

FIGURE 5. On the left: image u obtained with the proposed method . On the right: (top to bottom) zoom image of the recovered image u, noisy image I_n, and original image I_o.

The absolute difference between I_n and I_o and between u and I_o is shown in Figure 6. The improvements obtained with the proposed variational method are evident, most of the artifacts were significantly reduced. In this example the optimal parameters $\theta = 0.05$ and $\alpha = 1.2$ were found. Note that when compared with Example 1 the value α, associated with the denoising total

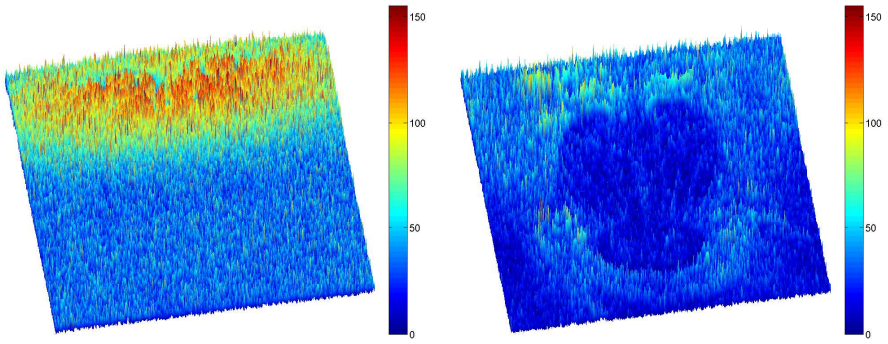

FIGURE 6. From left to right: image of the absolute difference between the original image I_o and the noisy image I_n and between the original image I_o and the recovered image u.

variation term, is much larger. This is expected since in Example 2 the level of Gaussian noise was increased.

The reference images I_r used in Example 2 and Example 3 are indicated by a dashed blue box in the noisy images of Figure 1 and Figure 4. Observe that these sub-images are afterwards resized to the images I_n dimensions.

3.3. Example 3. We observe that in these synthetic examples a good estimation of the parameter $\beta(x)$ is easily obtained. However, this may not be the case in real-world conditions. Having this issue in mind, we test in the next example the robustness of the proposed method with respect to $\beta(x)$. We consider again Example 2, but now we use a rough estimation of the parameter $\beta(x)$ in our variational model. The new parameter $\beta(x)$ and the recovered image u are shown in Figure 7. As can be seen, the image u obtained with this rough $\beta(x)$ is comparable with the one obtained in Example 2, where a more accurate estimation of $\beta(x)$ was used. Nevertheless, as highlighted in Figure 8, the results are not as precise as before.

4. Conclusion

In this work a variational image correction model was proposed and tested. Our model allows the automatic correction of common image related artifacts, namely, noise and illumination imbalance. The numerical results presented illustrate the applicability and efficiency of the proposed methodology. The correction of these type of problems is of major importance, for instance, on medical images [3]. As future work, we plan to extend the proposed model

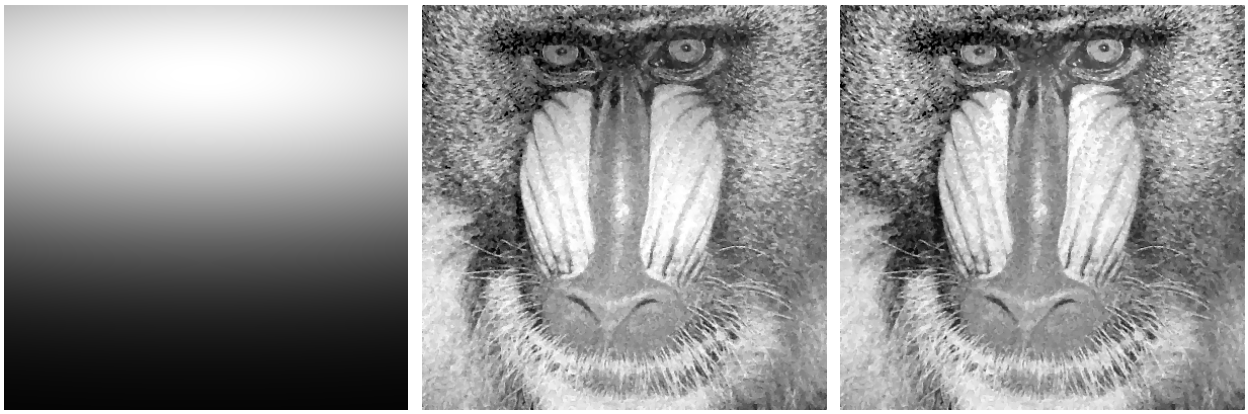

FIGURE 7. From left to right: new rough parameter $\beta(x)$, image u obtained with rough $\beta(x)$, and image u obtained in Example 2 with precise $\beta(x)$.

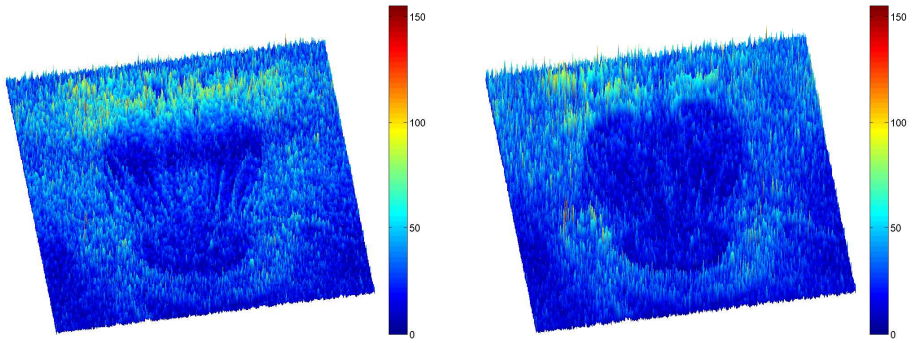

FIGURE 8. From left to right: image of the absolute difference between the original image I_o and the recovered image u obtained with rough and precise $\beta(x)$, respectively.

to color images and to perform more tests in real medical and remote sensing images. Another issue that should be addressed is the development of an automatic procedure to select the parameter $\beta(x)$.

References

[1] N. Bonneel, J. Rabin, and G. Peyré. Sliced and Radon Wasserstein barycenters of measures. *Journal of Mathematical Imaging and Vision*, 51:22–45, 2015.

[2] T. F. Chan and J. Shen. *Image processing and analysis: variational, PDE, wavelet, and stochastic methods*. SIAM, 2005.

[3] I. N. Figueiredo, C. Leal, L. Pinto, P. N. Figueiredo, and R. Tsai. An elastic image registration approach for wireless capsule endoscope localization. *(unpublished) https://arxiv.org/abs/1504.06206*, 2015.

[4] R. Kimmel, M. Elad, D. Shaked, R. Keshet, and I. Sobel. A variational framework for retinex. *International Journal of computer vision*, 52(1):7–23, 2003.
[5] X. Lan, H. Shen, L. Zhang, and Q. Yuan. A spatially adaptive retinex variational model for the uneven intensity correction of remote sensing images. *Signal Processing*, 101:19–34, 2014.
[6] E. H. Land and J. J. McCann. Lightness and retinex theory. *Journal of the Optical Society of America*, 61(1):1–11, 1971.
[7] H. Li, L. Zhang, and H. Shen. A perceptually inspired variational method for the uneven intensity correction of remote sensing images. *IEEE Transactions on Geoscience and Remote Sensing*, 50(8):3053–3065, 2012.
[8] J. Liu, B. D. Froese, A. M. Oberman, and M. Xiao. A multigrid scheme for 3D Monge–Ampère equations. *International Journal of Computer Mathematics*, pages 1–17, 2016.
[9] A.J. McCollum and W.F. Clocksin. Multidimensional histogram equalization and modification. In *Image Analysis and Processing, 2007. ICIAP 2007. 14th International Conference on*, pages 659–664. IEEE, 2007.
[10] J. Morovic and P.-L. Sun. Accurate 3D image colour histogram transformation. *Pattern Recognition Letters*, 24(11):1725–1735, 2003.
[11] N. Papadakis, E. Provenzi, and V. Caselles. A variational model for histogram transfer of color images. *IEEE Transactions on Image Processing*, 20(6):1682–1695, 2011.
[12] F. Pitié, A. C. Kokaram, and R. Dahyot. Automated colour grading using colour distribution transfer. *Computer Vision and Image Understanding*, 107(1):123–137, 2007.
[13] J. Rabin and G. Peyré. Wasserstein regularization of imaging problem. In *18th IEEE International Conference on Image Processing, Brussels*, pages 1541–1544, 2011.
[14] L. Rudin, S. Osher, and E. Fatemi. Nonlinear total variation based noise removal algorithms. *Physica D: Nonlinear Phenomena*, 60(1-4):259–268, 1992.
[15] C. Villani. *Topics in optimal transportation*. Number 58. American Mathematical Soc., 2003.
[16] C. R. Vogel. *Computational methods for inverse problems*. SIAM, Philadelphia, USA, 2002.

Isabel Narra Figueiredo
CMUC, Department of Mathematics, University of Coimbra, Portugal.
E-mail address: isabelf@mat.uc.pt
URL: http://www.mat.uc.pt/∼isabelf/

Luís Pinto
CMUC, Department of Mathematics, University of Coimbra, Portugal.
E-mail address: luisp@mat.uc.pt

Gil Gonçalves
Institute for Systems Engineering and Computers at Coimbra (INESCC) and the Department of Mathematics, University of Coimbra, Portugal.
E-mail address: gil@mat.uc.pt

Björn Engquist
Department of Mathematics and ICES, The University of Texas at Austin, Austin, USA.
E-mail address: engquist@math.utexas.edu
URL: https://www.ices.utexas.edu/people/160/